ELSEVIER

Coordination Chemistry Reviews 226 (2002) 113–124

COORDINATION
CHEMISTRY REVIEWS

www.elsevier.com/locate/ccr

Cocrystallites consisting of metal macrocycles with fullerenes

Tomohiko Ishii *, Naoko Aizawa, Ryo Kanehama, Masahiro Yamashita *,
Ken-ichi Sugiura, Hitoshi Miyasaka

Department of Chemistry, Graduate School of Science, Tokyo Metropolitan University and PRESTO (JST), 1-1 Minamiohsawa, Hachioji, Tokyo 192-0397, Japan

Received 10 April 2001; received in revised form 11 September 2001; accepted 21 September 2001

Contents

Abstract

The cocrystallites that contain C_{60}, C_{70} and endohedral metallofullerenes with metal complexes of macrocycles are reviewed. Metal complexes of porphyrin cocrystallites with fullerenes form solids with remarkably close contact between the curved π surface of a fullerene and the planar π surface of a porphyrin, without the need for matching convex with concave surfaces. The structures of metal octaethylporphyrins (oeps) in C_{60}·Pd(II)(oep)·1.5C_6H_6, C_{60}·Cu(II)(oep)·2C_6H_6, C_{60}·Ag(II)(oep)·2C_6H_6 and C_{60}·2Ni(II)(oep)·2C_6H_5Cl reveal the remarkable *anti*-formed oep configurations, with the four ethyl groups of the metal oep portions lying on both the same and the opposite sides of the porphyrin plane toward the C_{60}. On the other hand, *syn*-formed metal oeps are observed in the many cases of metal oep compounds, suggesting that there is a face-to-face interaction between two adjacent oep planes. A new cocrystallite which exhibits a strong intermolecular interaction between fullerene C_{60} and the Co(tbp) is also reviewed, where tbp denotes a dianion of tetra(bis-*tert*-butylphenyl)porphyrin. The intermolecular interactions of the *anti*- and *syn*-formed metal oeps in the cocrystallites containing fullerenes are also described by DV-Xα molecular orbital calculation. © 2002 Elsevier Science B.V. All rights reserved.

Keywords: Fullerene C_{60}, C_{70} and endohedral metallofullerene; Macrocycles; Porphyrin oep and tpp; Fullerene cocrystallites; X-ray structural analysis; DV-Xα molecular orbital calculation

1. Introduction

For more than 10 years the syntheses and physical properties of C_{60} have been extensively investigated for the unique properties caused by their three-dimensional

---

* Corresponding authors. Tel.: +81-426-77-2550; fax: +81-426-77-2525.

E-mail addresses: mail@tishii.com (T. Ishii), yamashit@comp.metro-u.ac.jp (M. Yamashita).

0010-8545/02/$ - see front matter © 2002 Elsevier Science B.V. All rights reserved.
PII: S0010-8545(01)00442-8

shapes [1,2]. The ball-shaped fullerenes such as C_{60} and C_{70} are not appropriate to cocrystallize with planar molecules, and curving of the planar molecule to match the concave structure is required in order to fit to the ball-shaped fullerenes [3,4]. In some circumstances, there have been several reports of researchers obtaining curved surfaces that are able to encircle a fullerene by building complex structures from planar aromatic hydrocarbon units and other flat moieties. A number of concave molecules based on calixarenes [5], oxacalix[3]arenes [6], resorcina[4]arenes [7], γ-cyclodextrin [8], azacrown ethers [9], porphyrazine [10,11], cyclotriveratrylene [12], bis(ethylenedithio)-tetrathiafulvalene [13] and tetramethylenedithiodimethyl-tetrathiafulvalene [14] have been reported to form cocrystallites with C_{60} and C_{70}. Concerning the macrocyclic metal compounds, concave structures based on non-planar molecules (Fig. 1(a)) such as Ni(omtaa) [15], Ni(tmtaa) [16] and Cu(tmtaa) [17] (omtaa = octamethyldibenzotetraazaannulenato, tmtaa = tetramethyldibenzo-tetraazaannulenato) have also been required in order to form cocrystallites with C_{60}. The first observation of a porphyrin–fullerene close approach was reported by Sun et al. [18]. Recently, metal complexes of octaethylporphyrin (Fig. 1(b)) (oep, which is the dianion of octaethylporphyrin) cocrystallites with C_{60} have been reported [19] to form solids with remarkably close contact, that is, an interaction takes place between the curved π surface of a fullerene with the planar π surface of a porphyrin, without the need for matching convex with concave surfaces [20]. In addition, unique cocrystallites of C_{60} and C_{70} fullerenes with tpps (tpp is a dianion of tetraphenylporphyrin) have also been reported [20].

Here, we review the metal complexes of macrocycles such as tetraazaannulene (taa), *syn*- and *anti*-formed [21] oep (Fig. 2), and Co(tbp) (tbp = 5,10,15,20-tetrakis[3,5-(bis-*tert*-butyl)phenyl]porphyrin) cocrystallized with C_{60} and C_{70}. The orientation of the eight terminal ethyl groups on the metal oep is supposed to be very important in order to make a cocrystallite of the curved surfaced fullerenes with the planar surfaced porphyrin. There is also the possibility of a strong interaction between fullerenes, including an air sensitive endohedral metallofullerene, and the metal oeps. We also describe the relationship between the configuration and the energy levels in comparison between the *syn*- and *anti*-formed oeps by means of DV-Xα molecular orbital calculation.

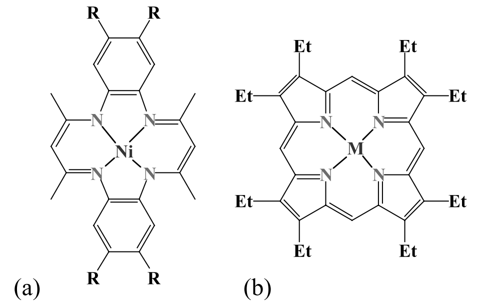

Fig. 1. (a) (5,7,12,14-tetramethyldibenzo[*b*,*i*][1,4,8,11]tetraazacyclotetradecine)nickel(II) (R = H) (Ni(II)(tmtaa)). (5,14-dihydro-2,3,6,8,11,12,15,17-octamethyldibenzo[*b*,*i*][1,4,8,11]tetraazacyclotetradecine) nickel(II) (R = Me) (Ni(II)(omtaa)). (b) 2,3,7,8,12,13,17,18-Octaethyl-21*H*,23*H*-porphine metallate(II) (M(II)(oep), M = Zn, Ru(CO), Pd, Cu, Ag, Ni, etc.).

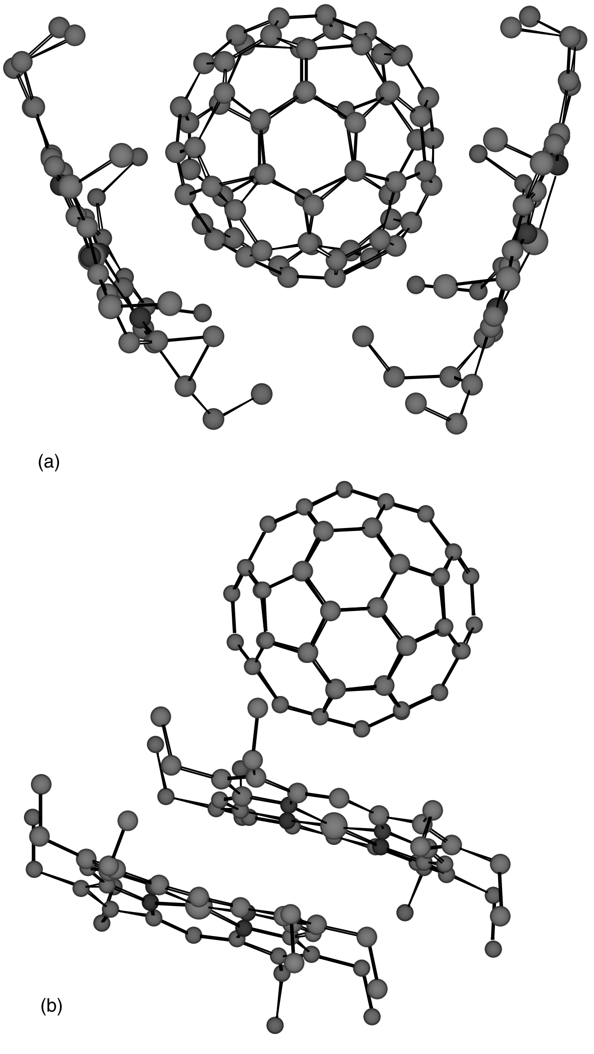

Fig. 2. Configurations of metal oeps observed in cocrystallines with C_{60}; (a) *syn*-formed Zn(II)(oep) in $C_{60}\cdot 2Zn(II)(oep)\cdot 2C_6H_6$ and (b) *anti*-formed Cu(II)(oep) in $C_{60}\cdot Cu(II)(oep)\cdot 2C_6H_6$.

2. Cocrystallites consisting of metal macrocycles with fullerenes

The compounds reported here were obtained in a form suitable for single-crystal X-ray diffraction.

2.1. Metal tetraazaannulene complexes, C_{60}·M(taa) and C_{70}·M(taa) (taa = tetraazaannulenato)

Concerning the macrocyclic metal compounds, the complementary of curvature based on non-planar molecules such as Ni(omtaa), Ni(tmtaa) and Cu(tmtaa) could be argued as assisting the host–guest interactions in order to form cocrystallites with C_{60} and C_{70}. The M(taa) molecules (Fig. 1(a)) are curved, implying that there is little change of the radius of curvature on complexation with the ball-shaped C_{60} and C_{70}. Among them, the C_{60}·Ni(tmtaa) complex is one of the most popular cocrystallites consisting of annulene with C_{60} [16]. In this compound, Ni(tmtaa) has two divergent concave surfaces in a saddle shape arrangement which arises from the otherwise unfavorable interactions between the methyl groups and the adjacent H-atoms on the aromatic rings, as shown in Fig. 3 [16]. It can act as a divergent heterotropic receptor toward C_{60}. In the structure of C_{60}·Ni(tmtaa), two host molecules shroud the fullerene such that a fullerene is in the saddle of one Ni(tmtaa) molecule with the methyl groups directed towards it and in the opposite saddle of another Ni(tmtaa) molecule, the overall host–guest contacts form a continuous zigzag array (Fig. 3) with the fullerenes forming a corrugated two dimensional sheet [16]. Cu(II) [17] and Zn(II) [20] tmtaa molecules similarly bind fullerene and are isostructural with the Ni(II) analogue. For omtaa a 1:1 complex is formed with C_{60} isolated as $[C_{60}\cdot Ni(omtaa)](CS_2)_2$ [15]. The extended supramolecular array is based on linear chains of close contact C_{60} molecules, and linear chains of π-stacked alternating molecules of C_{60} and Ni(omtaa) with adjacent chains running in opposite directions and thus canceling out dipole moments. The same macrocycle forms a 1:1 complex with C_{70} which is isostructural with the C_{60} complex of Ni(tmtaa), i.e. zigzag alternating C_{70}–Ni(omtaa) chains with corrugated sheets of close contact C_{70} molecules [22]. In all of these Ni(II) macrocycle structures there are no significant contacts between the metal centers and the fullerenes.

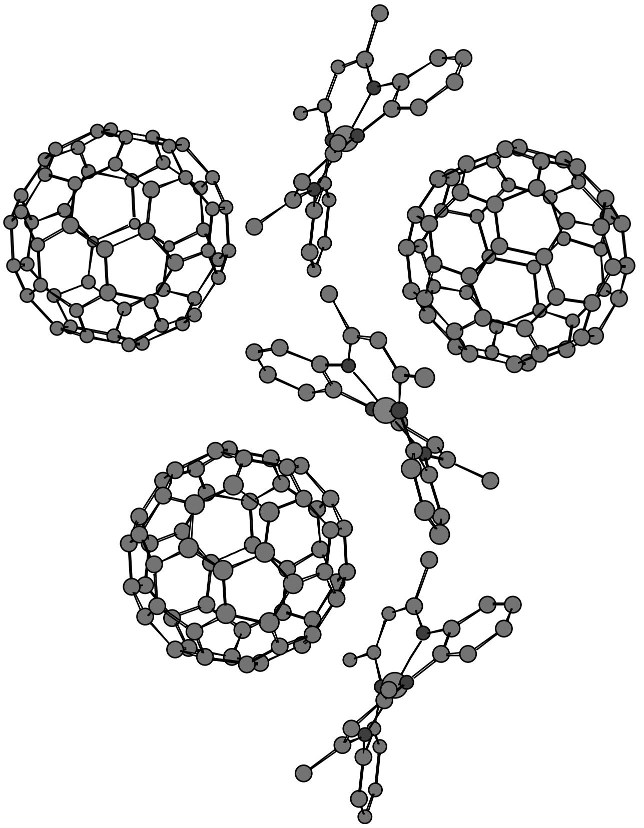
Fig. 3. The continuous zigzag array of C_{60}·Ni(tmtaa).

2.2. The syn-formed metal oep complexes with fullerenes (oep = dianion of octaethylporphyrin)

One of the typical complexes consisting of *syn*-formed metal oep with fullerene is $C_{60}\cdot Ru(II)(CO)(oep)\cdot 2C_6H_5CH_3$ [23]. The centric unit cell of the *Pnma* space group in the compound consists of a C_{60} molecule, one ruthenium carbonyl oep and two solvent molecules of toluene, as shown in Fig. 4. Within this unit cell the fullerene is positioned symmetrically between the two Ru(II)(CO)(oep) units. The distance from the ruthenium atom to this C–C bond is 2.75 Å. The Ru–C distances are 2.83(3)–2.86(3) Å. These distances are short enough for interaction between neighboring fullerenes.

The cocrystallite consists of the *syn*-formed oep and C_{60}. These eight ethyl groups of the ruthenium carbonyl oep portion lie on the same side of the porphyrin, toward the fullerene. In this porphyrin a carbonyl ligand is located on the opposite side of the planar porphyrin from the eight ethyl groups. This structural feature is very similar to that reported for $C_{60}\cdot Fe(III)Cl(oep)\cdot 2CHCl_3$ [19].

In addition to these fullerene/porphyrin interactions, there are significant porphyrin/porphyrin contacts with either pairwise or face-to-face contact. The combination of fullerene/porphyrin and porphyrin/porphyrin contacts produces a 'two slipped potlids-like' structure. The two slipped potlids arrangement is facilitated by the positioning of all of the ethyl groups on the same side of the porphyrin from the adjacent porphyrin.

Another example of a complex consisting of *syn*-formed metal oep with fullerene is $C_{60}\cdot 2Zn(II)(oep)\cdot 2C_6H_6$ [23]. The asymmetric unit cell of the $P2_12_12_1$ space group in the compound consists of a C_{60} molecule, two zinc oeps and two solvent molecules of benzene. Within this unit cell, the fullerene is positioned symmetrically between the two Zn(II)(oep) units. The distance from the zinc atom to this C–C bond is 2.97 Å. The Zn–C distances are 2.98(3)–3.20(4) Å. This structural feature is very similar to that reported in $C_{60}\cdot 2Zn(II)(oep)\cdot 2CH_2Cl_2$ [19].

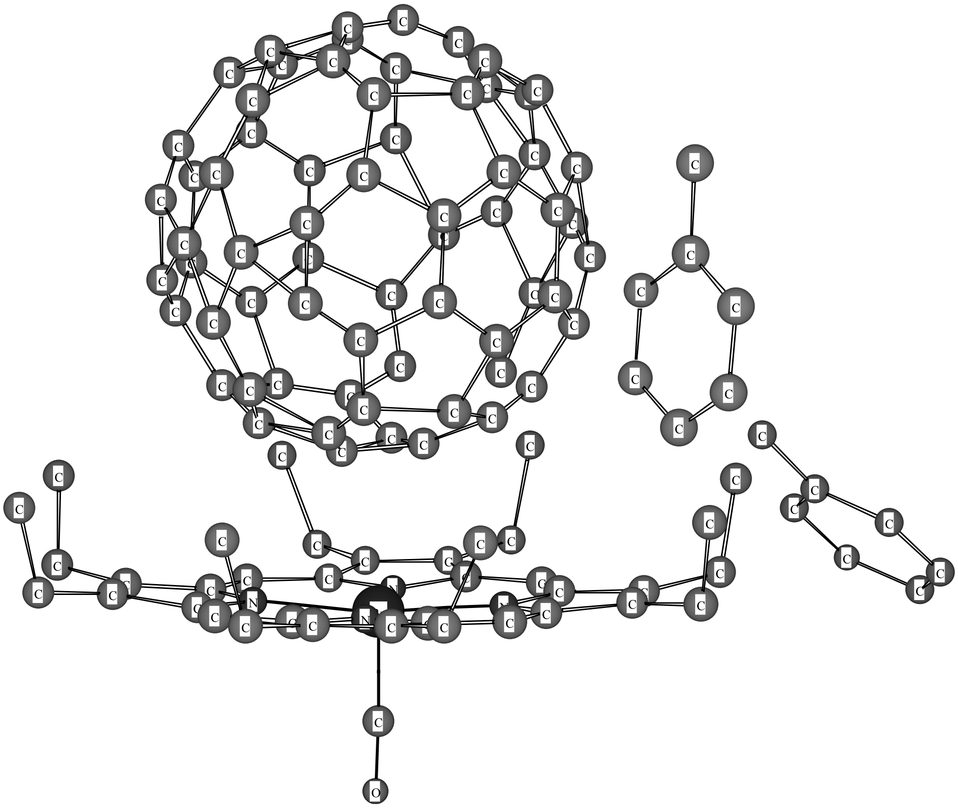

Fig. 4. A drawing that shows the molecular packing in C_{60}·Ru(II)(CO)(oep)·$2C_6H_5CH_3$.

Fig. 5 shows a drawing of the molecular packing that makes clear the neighboring fullerene toward the eight ethyl groups of these zinc oep molecules. In addition to these fullerene/porphyrin interactions, there are significant porphyrin/porphyrin contacts with pairwise or face-to-face contact. It is expected that the face-to-face porphyrin/porphyrin contact is greater in the fullerene cocrystallites than it is in the pristine Zn(II)(oep) compound [24,25]. Other complexes with *syn*-formed metal oep, such as C_{60}·2Co(II)(oep)·$CHCl_3$, C_{60}·2Zn(II)(oep)·$CHCl_3$, $C_{60}O$·2Co(II)(oep)·$CHCl_3$ and C_{60}·ClFe(III)-(oep)·$CHCl_3$ have been reported [19] and are summarized in Table 1.

An isomorphous series of cocrystallites with C_{70}, i.e. C_{70}·Co(II)(oep)·C_6H_6·$CHCl_3$, C_{70}·Ni(II)(oep)·C_6H_6·$CHCl_3$ and C_{70}·Cu(II)(oep)·C_6H_6·$CHCl_3$, has also been reported [19]. The C_5 axis of the fullerene makes an angle of 16.4° with the porphyrin plane in C_{70}·Co(II)-(oep)·C_6H_6·$CHCl_3$, 16.2° in C_{70}·Ni(II)(oep)·C_6H_6·$CHCl_3$ and 16.6° in C_{70}·Cu(II)(oep)·C_6H_6·$CHCl_3$. In the series C_{70}·Co(II)(oep)·C_6H_6·$CHCl_3$, C_{70}·Ni(II)(oep)·C_6H_6·$CHCl_3$ and C_{70}·Cu(II)(oep)·C_6H_6·$CHCl_3$, the closest contacts between C_{70} molecules are 3.486, 3.438, and 3.395 Å, respectively. The structure of the cocrystallite is shown for the complex consisting of VO(oep) with C_{70}, C_{70}·VO(oep)·C_6H_6·H_2O in Fig. 6 [26]. In this example the *syn*-formed configuration of VO(oep) can be observed even though two adjacent VO(oep) planes are separated enough for the face-to-face contact to disappear. The VO(oep) molecules play a role as template to line up the fullerene C_{70} molecules in a row, as shown in Fig. 7. The intermolecular distances between nearest C_{70} molecules are fairly short, 2.94–3.05 Å, and therefore there is a possibility for this to be a high conducting material. Such a short distance between C_{70}

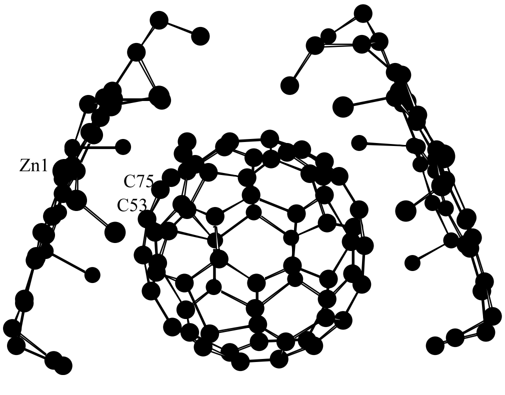

Fig. 5. A view of the fullerene/porphyrin units in C_{60}·2Zn(II)(oep)·$2C_6H_6$. The benzene molecules are omitted in this drawing.

Table 1

Fullerene	Macrocycle	Composition of cocrystallite	Ref.
C_{60}	Annulene	C_{60}·Ni(tmtaa)	[16]
C_{60}	Annulene	C_{60}·Ni(omtaa)·2CS_2	[15]
C_{60}	Annulene	C_{60}·Cu(tmtaa)	[17]
C_{60}	Porphyrazine	C_{60}·2Cu(Pz)	[11]
C_{60}	Porphyrazine	C_{60}·Ni(Pz)	[11]
C_{60}	tpp	H_2(tpp)·C_{60}·3$C_6H_5CH_3$	[20]
C_{60}	tpp derivative	$H_2T_{3,5\text{-dibutyl}}PP$·$C_{60}$	[20]
C_{60}	tpp derivative	$H_2T_{3,5\text{-dimethyl}}PP$·1.5$C_{60}$ ·2$C_6H_5CH_3$	[20]
C_{60}	tpp derivative	$H_2T_{piv}PP$·C_{60}	[20]
C_{60}	tpp derivative	C_{60}·Co(II)(tbp)	[33]
C_{60}	*syn*-oep	C_{60}·2Co(II)(oep)·$CHCl_3$	[19]
C_{60}	*syn*-oep	C_{60}·2Zn(II)(oep)·$CHCl_3$	[19]
C_{60}	*syn*-oep	$C_{60}O$·2Co(II)(oep)·$CHCl_3$	[19]
C_{60}	*syn*-oep	C_{60}·ClFe(III)(oep)·$CHCl_3$	[19]
C_{60}	*syn*-oep	C_{60}·Ru(II)(CO)(oep) ·2$C_6H_5CH_3$	[23]
C_{60}	*syn*-oep	C_{60}·2Zn(II)(oep)·2C_6H_6	[23]
C_{60}	*anti*-oep	C_{60}·Pd(II)(oep)·1.5C_6H_6	[23]
C_{60}	*anti*-oep	C_{60}·Cu(II)(oep)·2C_6H_6	[23]
C_{60}	*anti*-oep	C_{60}·Ag(II)(oep)·2C_6H_6	[30]
C_{60}	*anti*-oep	C_{60}·2Ni(II)(oep)·2C_6H_5Cl	[30]
C_{70}	Annulene	C_{70}·Ni(omtaa)	[22]
C_{70}	tpp	Zn(tpp)·C_{70}	[20]
C_{70}	tpp derivative	C_{70}·$H_2T_{3,5\text{-dimethyl}}PP$·4$C_6$-$H_5CH_3$	[20]
C_{70}	tpp derivative	$NiT_{4\text{-methyl}}PP$·2C_{70}·2C_6-H_5CH_3	[20]
C_{70}	*syn*-oep	C_{70}·Co(II)(oep) ·C_6H_6·$CHCl_3$	[19]
C_{70}	*syn*-oep	C_{70}·Ni(II)(oep) ·C_6H_6·$CHCl_3$	[19]
C_{70}	*syn*-oep	C_{70}·Cu(II)(oep) ·C_6H_6·$CHCl_3$	[19]
C_{70}	*syn*-oep	C_{70}·VO(oep)·C_6H_6·H_2O	[26]
$NSc_3@C_{80}$	*syn*-oep	$NSc_3@C_{80}$·Co(II)(oep) ·1.5$CHCl_3$·0.5C_6H_6	[41]
$NErSc_2@C_{80}$	*syn*-oep	$NErSc_2@C_{80}$·Co(II)(oep) ·0.3$CHCl_3$·1.5C_6H_6	[42]

molecules has not been observed previously in reports of C_{70}·Co(II)(oep)·C_6H_6·$CHCl_3$, C_{70}·Ni(II)(oep)·C_6H_6·$CHCl_3$ and C_{70}·Cu(II)(oep)·C_6H_6·$CHCl_3$ [19].

2.3. Crystal structure of C_{60} cocrystallites with anti-formed metal oep

The first examples of cocrystallites which contain C_{60} with the *anti*-formed metal complexes of oep are reported for C_{60}·Pd(II)(oep)·1.5C_6H_6 and C_{60}·Cu(II)(oep)·2C_6H_6 [23]. These two compounds are almost isomorphous structures, but the space groups are different, acentric $P1$ and centric $P\bar{1}$ for the palladium and the copper compounds, respectively. The unit cell in each compound consists of a C_{60} molecule, one metal oep and several molecules of benzene, as shown in Fig. 8 for C_{60}·Pd(II)(oep)·1.5C_6H_6. Within this unit cell in Fig. 8, the fullerene is positioned symmetrically between the two Pd(II)(oep) units, and the fullerene is too far from the atoms of the Pd(II)(oep) for any covalent bonding between them. The planar structure of the metal porphyrin still remains in the cocrystallite with C_{60}, in contrast to other M(tmtaa) and M(omtaa) macrocyclic complexes with C_{60} which have been reported to have the saddle shaped structure. It is supposed that interaction takes place between the curved π

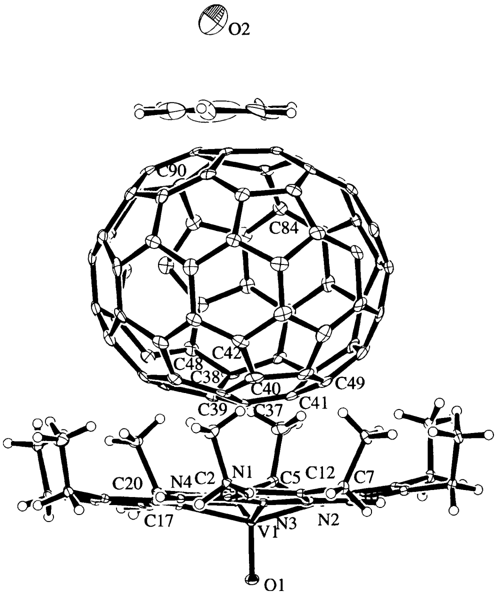

Fig. 6. Atom numbering in C_{70}·VO(oep)·C_6H_6·H_2O with 50% thermal ellipsoids.

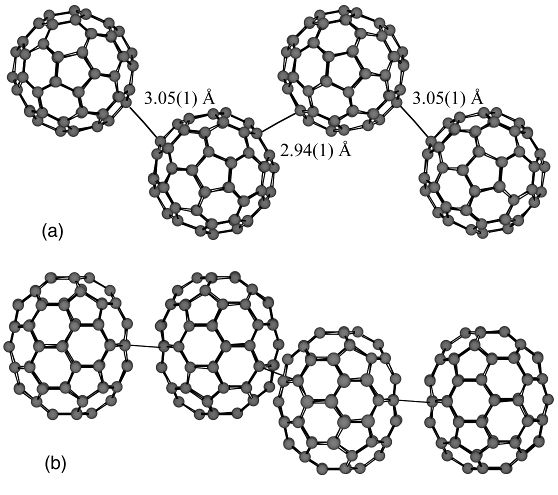

Fig. 7. The molecular packing of fullerene C_{70} molecules in C_{70}·VO(oep)·C_6H_6·H_2O; (a) top view and (b) side view. Only one set of four orientations of the C_{70} units is shown.

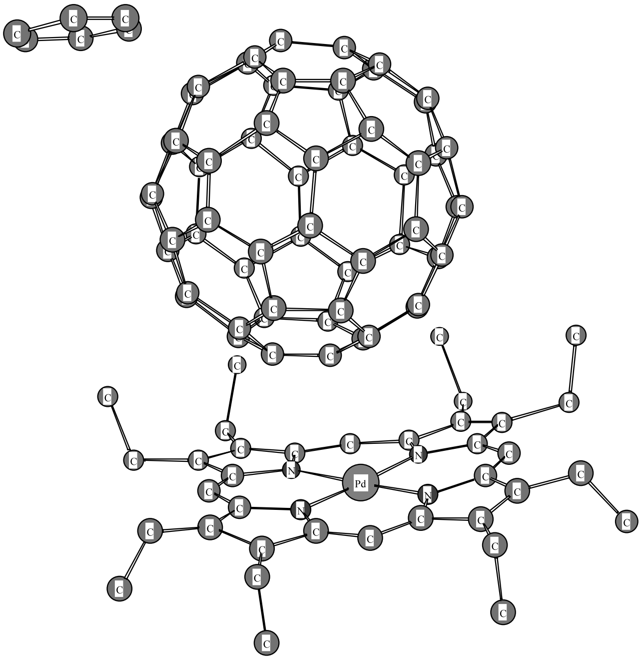

Fig. 8. A drawing that shows the molecular packing in C_{60}·Pd(II)(oep)·$1.5C_6H_6$.

surface of the fullerene with the planar π surface of the porphyrin, without the need for matching convex with concave surfaces. In general, it has been thought that C_{60} is centered over the metal atom of complexes via the electron-rich 6:6 ring-juncture C–C bonds, which are provided with the filled h_u orbitals, in close approach to the plane of the metal complex core. On the other hand, in the closest approach to the palladium atom the fullerene is peculiarly positioned involving the 5:6 ring junction, which denotes π-antibonding between the carbon atoms (i.e. the Pd(1)···[C(11)–C(135) bond] in Fig. 9). The shortest distance from the palladium atoms to the C–C bond is 3.01–3.04 Å (Pd(1)···[C(11)–C(135)]). In general, the closest contact between C_{60} and the central metal atom in the cocrystallites with M(tmtaa) is 3.18–3.37 Å. On the other hand, this value for the copper compound is 3.007 Å. While these distances are too long for a coordinate bond, they are shorter than the normal van der Waals contact seen between neighboring fullerenes (greater than 3.2 Å) [27].

A characteristic feature is that these cocrystallites consist of the *anti*-formed metal oeps and C_{60}, that is, the four ethyl groups of both metal oep portions lie on

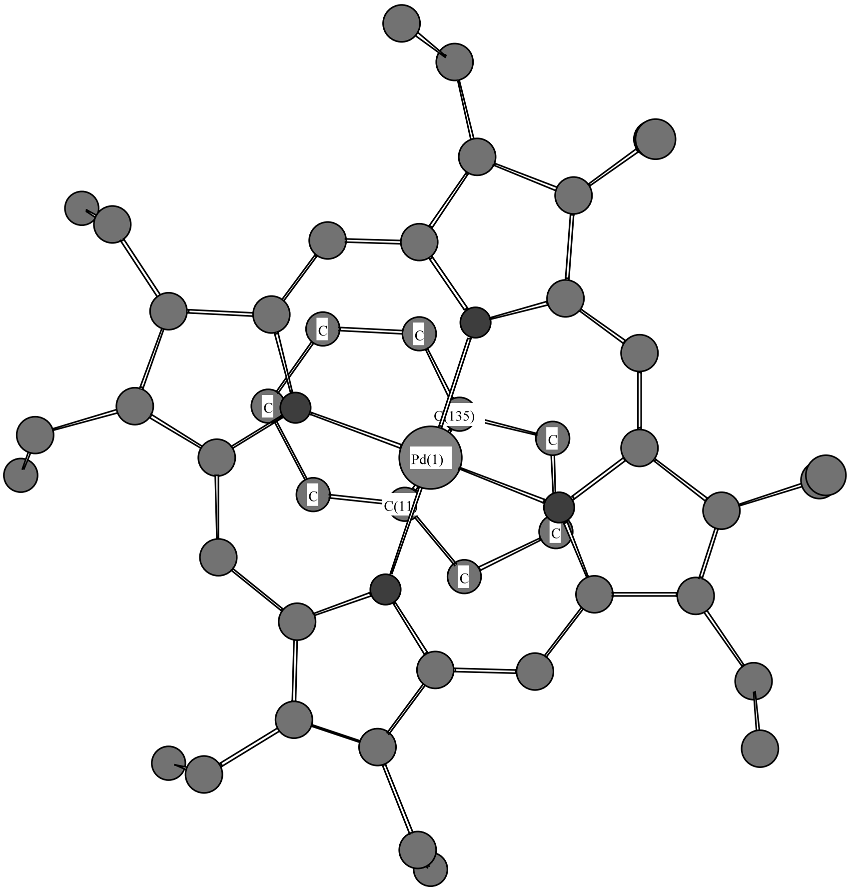

Fig. 9. The 5:6 carbon ring junction in the closest approach to the palladium atom in C_{60}·Pd(II)(oep)·$1.5C_6H_6$ shown from the opposite side to the fullerene. The carbon atoms on fullerene except the (C labeled) atoms involving the 5:6 ring junction are omitted to guide the eye.

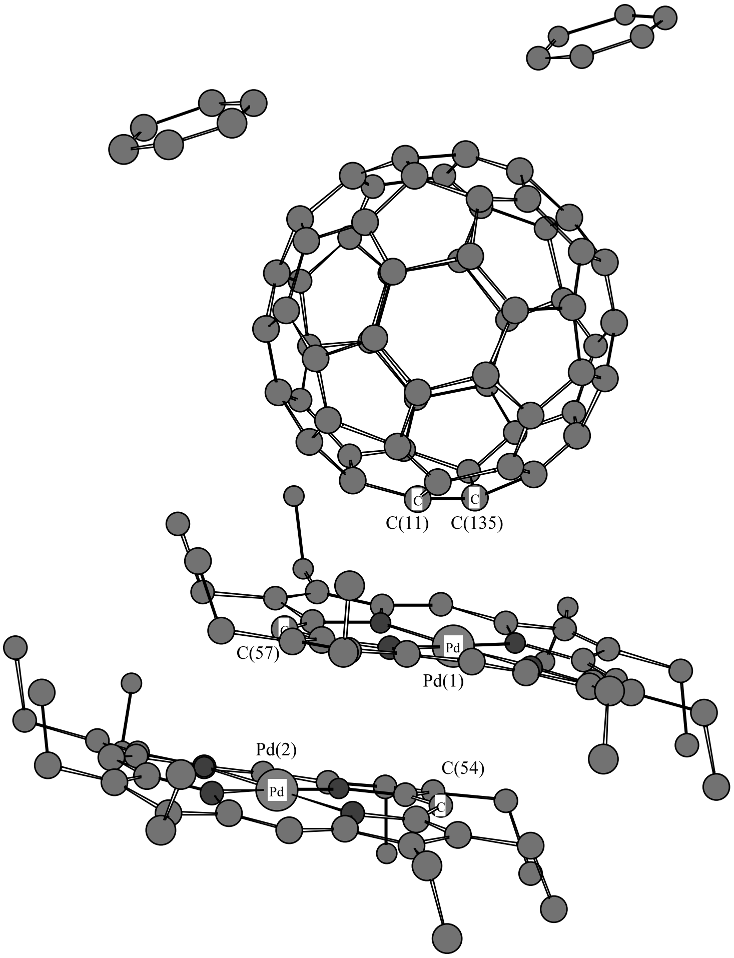

Fig. 10. A view of the fullerene/porphyrin units in C_{60}·Pd(II)(oep)·1.5C_6H_6 with 50% thermal ellipsoids.

the same side of the porphyrin toward the fullerene, and the other four ethyl groups lie on the opposite side of the porphyrin from the fullerene. The distances from the fullerene to the ethyl hydrogen atoms span the range 2.5–2.7 Å.

In addition to these fullerene/porphyrin interactions, there are significant *anti*-formed porphyrin/porphyrin contacts with pair-wise character. The combination of fullerene/porphyrin and porphyrin/porphyrin contacts produces a 'soccer ball on stackable chairs-like' structure, as shown in Fig. 10. The pair-wise porphyrin–porphyrin distances are Pd(1)···C(54), 3.30(1) Å; Pd(2)···C(57), 3.23(2) Å. The porphyrin–porphyrin distance of the Cu compound is shorter still, that is, 3.177(2) Å. Thus, the two porphyrin planes are within van der Waals contact of each other.

The core molecular geometries of the metal oep in C_{60}·Pd(II)(oep)·1.5C_6H_6 and C_{60}·Cu(II)(oep)·2C_6H_6 are very similar to those that are found in pristine Pd(II)(oep) and Cu(II)(oep) compounds [28,29]. Notice from these results that the pairwise porphyrin/porphyrin contacts are greater in the fullerene cocrystallites than they are in pristine Pd(II)(oep) and Cu(II)(oep) compounds. Other complexes with *anti*-formed metal oep, such as C_{60}·Ag(II)(oep)·2C_6H_6 [30] and C_{60}·2Ni-(II)(oep)·2C_6H_5Cl [31] have been reported and summarized in Table 1.

2.4. Strong intermolecular interaction in a cocrystallite with cobalt tetrakis(di-*tert*-butylphenyl)porphyrin

Unique cocrystallites of C_{60} and C_{70} fullerenes with tetraphenylporphyrins (tpps) have also been reported [20]. However, few cocrystallites of any metal tpp complexes with C_{60}, except the η^2-C_{60} cocrystallite with tetrakis(pentafluorophenyl)borate [32], have been synthesized. In the case of the metal tpp, only the cocrystallite with C_{70} has been reported [20]. In metal tpps, a modification of the structure of the terminal phenyl groups is regarded to be very important in order to make the cocrystallite of the curved C_{60} surface match with the planar surface of the porphyrin. So, we synthesized the cobalt complex of 5,10,15,20-tetrakis[3,5-(bis-*tert*-butyl)phenyl]porphyrin (tbp) (Fig. 11) cocrystallized with C_{60}, according to the strategy of structural modification by the addition of bis-*tert*-butyl groups into the tpp [33].

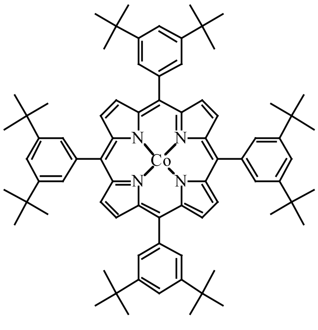

Co(tbp)

Fig. 11. 5,10,15,20-Tetrakis[3,5-(bis-*tert*-butyl)phenyl]porphyrin cobalt(II) (Co(II)(tbp)).

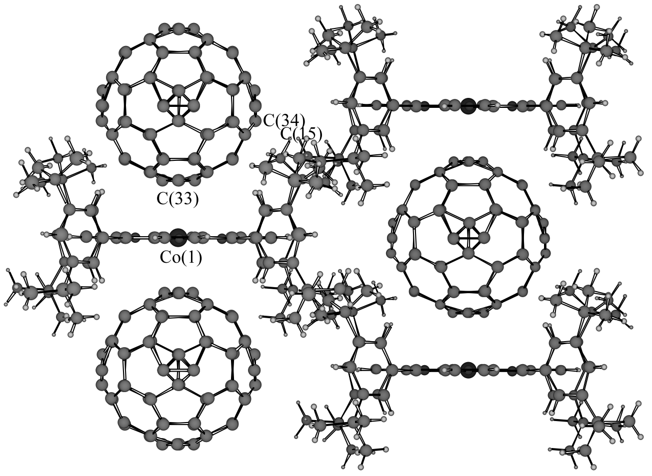

Fig. 13. Crystal Structure of Co(II)(tbp)·C_{60} viewed along the *a*-axis.

The unit cell in this compound consists of a C_{60} molecule and a Co(II)(tbp), as shown in Figs. 12 and 13. Within this unit cell, the Co(II)(tbp) is positioned symmetrically between two fullerene units and the fullerene is very close to the atoms of the Co(II)(tbp), allowing for the possibility for covalent bonding between them. The fullerene is caught by two porphyrin planes from top and bottom. In addition, the fullerene is also surrounded by the four porphyrins placed side by side. The fullerene is located in the position of closest approach to the centered metal atom, which involves an electron-rich π-bonding 6:6 carbon ring junction (hexagon–hexagon junction). The C_4 symmet-

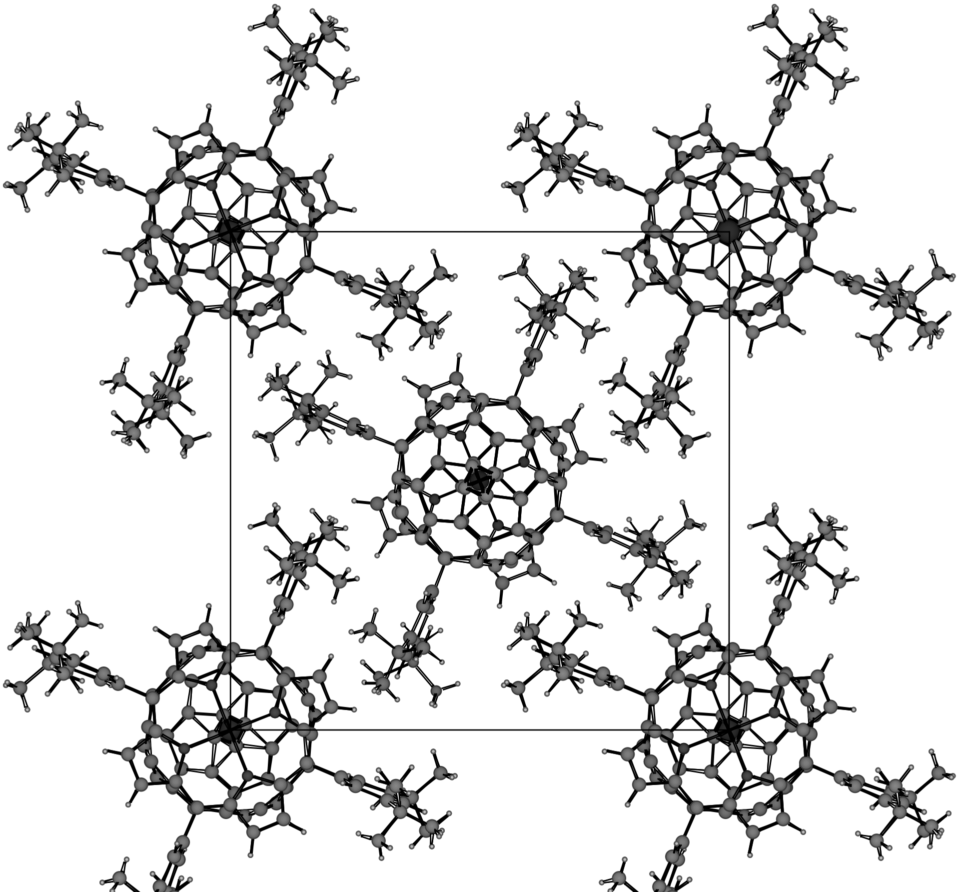

Fig. 12. Structure of Co(II)(tbp)·C_{60} viewed along the *c*-axis.

rical disorder of the carbon atoms on C_{60} is observed. The six carbon atoms, whose occupancy is 0.5, are disordered in the six octahedral points on the C_{60} framework. Such a phenomenon is explained by the two orientations at 90° relative to each other which are refined with 50% occupancy factor [34,35]. The C_{60} molecule belongs to the icosahedral point group and its cascade symmetry point group, (i.e. D_{5d}, D_{3d}, D_{2h} etc.), but it does not belong to the C_4 symmetry group. Each individual fullerene molecule does not possess C_4 symmetry. On the other hand, the Co(II)(tbp) molecule belongs to the typical C_4 point group. This unusual C_4 symmetry of C_{60} observed in the Co(II)(tbp)·C_{60} cocrystallite is related to the strong intermolecular interaction between the C_{60} and the C_4 symmetric molecule of Co(II)(tbp).

The closest distance between the cobalt atom and a carbon atom on C_{60} is 2.61 Å (i.e. Co(1)···C(33)). On the other hand, the closest distance from the *tert*-butyl group of Co(II)(tbp) to the carbon atom on C_{60} is 3.50(1) Å (i.e. C(15)···C(34)). The X-ray structural analysis of this compound was carried out at room temperature. Over a dozen porphyrin/fullerene or metalloporphyrin/fullerene structures have been reported using lower temperatures in order not only to optimize accuracy but also to conceal the imperfect C_{60} structures with large anisotropic thermal parameters. So far, none of the cocrystallites with fullerene have been determined with absolute atomic position for the crystal structure using X-ray analysis at room temperature, because it is very difficult to reduce the effect of the free rotation of the fullerene molecule at higher temperature. Therefore, this is the first example of an X-ray structural analysis performed at room temperature for a metal porphyrin cocrystallite with fullerene.

The structure of the Co(II)(tbp)·C_{60} cocrystallite is in the perfect ideal 3-D packing form with a highly C_4 symmetrical point group. The fullerene C_{60} molecule is caught tightly by six Co(II)(tbp) portions in the octahedral position of the C_{60}. As a result, X-ray structural analysis of this compound at room temperature can be done because the rotation of the C_{60} molecule is inhibited. The intermolecular distance between the C_{60} and Co(II)(tbp) molecules is quite short, i.e. 2.61 Å at room temperature and it decreases and reaches 2.58 Å at 83 K. This is the shortest length of all reported values, allowing for the possibility for covalent bonding between them. It is well known that the Co(II) ion in cobalt porphyrin complexes easily forms metal–carbon bonding along the axial direction. Such a short contact distance for metal–carbon bonding in cobalt porphyrin complexes has been reported in compounds such as CH_3COCH_2–Co(tpp) [36], $CHOCH_2$–Co(tpp) [37], CH_3–Co(oep) [38], C_2H_5–Co(oep) [39] and maleic anhydride–Co(tmp) [40] etc.

2.5. Endohedral metallofullerenes

Progress in exploring the chemical and physical properties of the endohedral fullerenes has been slowed by several factors: the low yields in which most endohedrals are produced, the frequent low solubility of the endohedrals, and the air sensitivity of some of these species. On the other hand, cocrystallites consisting of metal octaethylporphyrins with an endohedral metallofullerene can be obtained in a form suitable for single-crystal X-ray diffraction. The cocrystallites consisting of cobalt octaethylporphyrins with endohedral metallofullerenes (Fig. 14) have been reported by Olmstead et al. [41,42]. The structure of a mixed metal endohedral, $ErSc_2N@C_{80}$, has been determined by single-crystal X-ray diffraction at 90 K on $ErSc_2N@C_{80}$·Co(II)(oep)·$1.5C_6H_6$·$0.3CHCl_3$, which was obtained by diffusion of a solution of $ErSc_2N@C_{80}$ in benzene into a solution of Co(II)(oep) in chloroform. The structure of $ErSc_2N@C_{80}$ consists of a planar $ErSc_2N$ unit surrounded by an icosahedral C_{80} cage. The $ErSc_2N@C_{80}$ molecule sits at a site of crystallographic mirror symmetry. However, the C_{80} cage itself is orientationally disordered, and none of the 15 mirror planes of any one of the icosahedral cages coincides with the crystallographic mirror plane [43]. The N and Er atoms lie on a crystallographic mirror plane. The nominal Er–N distance is 2.089(9) Å and the Sc–N distance is, as expected, shorter, 1.968(6) Å. The Er–N–Sc angle is 119.1(3)° and the Sc–N–Sc angle is 121.3(6)°. The $ErSc_2N$ unit is planar within experimental error, with the sum of the two Er–N–Sc angles and the Sc–N–Sc angle equal to 359.6°. The Er and Sc thermal ellipsoids are elongated in directions which are indicative of motion of the $ErSc_2N$ group along the walls of the C_{80} cage. The Co(II)(oep) molecule resides on a crystallographic mirror plane which coincides with a molecular mirror plane that bisects the cobalt atom and two nitrogen atoms. The geometry of the Co(II)(oep) molecule is entirely normal. The Co–N distances (Co–N, 1.969(8), 1.985(6) and 1.976(7) Å) in $ErSc_2N@C_{80}$·Co(II)(oep)·$1.5C_6H_6$·$0.3CHCl_3$ are similar to those in Co(II)(oep) (Co–N, 1.967(3), 1.975(2) Å) [44], in C_{60}·2Co(II)(oep)·$CHCl_3$ (Co–N, 1.954(5)–1.985(6) Å), and in C_{70}·Co(II)(oep)·C_6H_6·$CHCl_3$ (Co–N, 1.964(5)–1.967(5) Å) [19]. The Co(II)(oep) molecule is positioned so that the ethyl groups of the porphyrin form a *syn*-formed octapoidal embrace about the C_{80} cage. The fullerene is too far from the cobalt atoms for any normal covalent bonding between them. The closest approaches of the cobalt atom to the C_{80} cage are 2.706 and 2.746 Å from the cobalt atom.

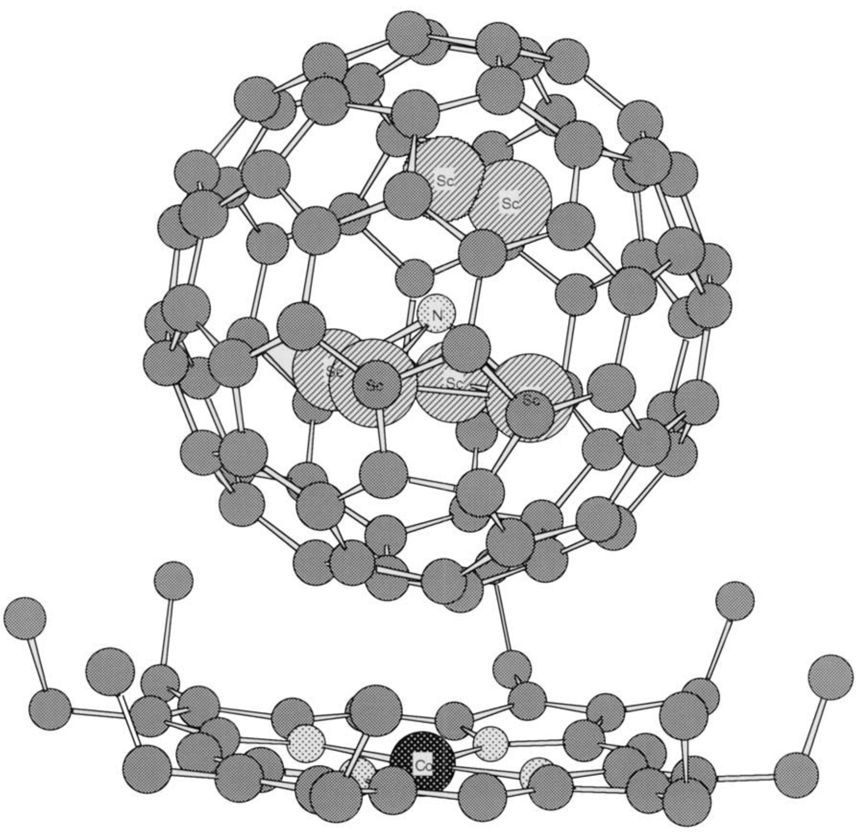

Fig. 14. A drawing that shows the molecular packing in $NSc_3@C_{80}\cdot Co(II)(oep)\cdot 1.5CHCl_3\cdot 0.5C_6H_6$. The Sc atoms are disordered with 0.5 of atomic occupancies.

3. DV-Xα calculations of *syn*- and *anti*-formed oeps in oep cocrystallites with C_{60}

A variety of configurations of pristine oeps are reported reflecting the structural flexibility of the terminal ethyl groups, but only the compounds containing C_{60} with the *syn*- or *anti*-formed metal oeps have been found. Therefore, the core molecular geometry of the metal oep found in the cocrystallite with C_{60} is not always similar to that found in the pristine metal oep compound. It is very important to discuss the difference of the stability between the *anti*- and the *syn*-formed metal oeps in the cocrystallites with C_{60}.

In order to discuss the stability of these complexes, the electronic level structures of *syn*- and *anti*-formed Zn(II)(oep), Ru(II)(oep) and Pd(II)(oep) molecules were calculated. The structural models for the DV-Xα molecular orbital calculation [45] for the *syn*-formed Zn(II)(oep), Ru(II)(oep) and *anti*-formed Pd(II)(oep) are derived from the results of the X-ray structural analyses, though the *syn*-formed Pd(II)(oep) and the *anti*-formed Zn(II)(oep) and Ru(II)(oep) are calculated by means of the MM2 method. The results of the electronic structures of these metal oeps are summarized in Fig. 15. From the result of this calculation, the energy levels of the *anti*-formed configurations are more stable in all cases than those of the *syn*-formed configurations. This result is consistent with the fact that the *anti*-formed configurations are observed in the pristine metal oeps. In the *syn*-formed compounds,

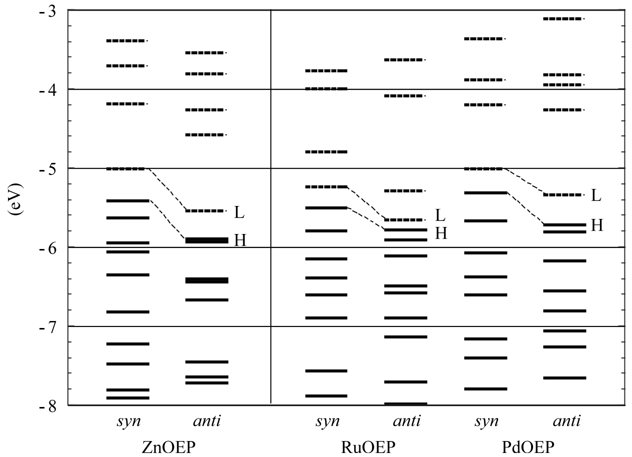

Fig. 15. DV-Xα calculation for electronic level structures comparing *syn*- and *anti*-formed Zn(II)(oep), Ru(II)(oep) and Pd(II)(oep). Solid and dashed lines indicate the electron occupied and unoccupied energy levels, respectively. The signs ‘H’ and ‘L’ denote the HOMO and LUMO energy levels, respectively. The basis functions of the centered metal for the metal oeps were employed up to the 4p orbital for Zn(II)(oep), and the 5p orbital for Pd(II)(oep) and Ru(II)(oep).

there is the possibility for the existence of strong face-to-face interaction between two adjacent metal oeps, resulting in the *syn*-formed oeps being observed transformed from the energetically stable *anti*-formed configuration. The distances between two adjacent porphyrin planes in the *syn*-formed compounds are shorter than those in the *anti*-formed compounds. This is the reason why *syn*-formed configurations are observed in the C_{60}·Zn(II)(oep)·2C_6H_6 and C_{60}·Ru(II)(CO)(oep)·2$C_6H_5CH_3$ compounds. In contrast, *anti*-formed configurations are observed in the C_{60}·Pd(II)(oep)·1.5C_6H_6, C_{60}·Cu(II)(oep)·2C_6H_6, C_{60}·Ag(II)(oep)·2C_6H_6 and C_{60}·2Ni(II)(oep)·2C_6H_5Cl compounds, suggesting that there is the possibility for the existence of a strong interaction between the C_{60} and the centered metal atoms of the metal oeps.

In C_{60}·Ru(II)(CO)(oep)·2$C_6H_5CH_3$ [23], a *syn*-formed configuration of the metal oep has been observed, in contrast to the fact that *anti*-formed configurations have been reported in several Ru(oep) compounds [46,47]. In this compound, a carbonyl ligand is located at the opposite side of the porphyrin plane from the eight ethyl groups. The face-to-face interaction between adjacent porphyrins is strengthened by these two carbonyl ligands, with the result that the *syn*-formed configuration of oep of the 'two slipped potlids-like' structure, which is also reported in C_{60}·ClFe(III)-(oep)·$CHCl_3$ compounds [19], is observed.

4. Experimental section

4.1. DV-Xα molecular orbital computational method

The non-relativistic DV-Xα calculation [48] was performed with the Slater exchange parameter, α, of 0.7 for all atoms and with 5000 DV sampling points, which provided a precision of less than 0.1 eV for valence electron energy eigenvalues. We employed the basis functions of the centered metal atom for the metal oeps up to the 4p orbitals for Cu and Zn, and the 5p orbitals for Pd and Ru, while those of the nitrogen, carbon and oxygen atoms were used up to the 2p orbitals. The calculations were carried out self-consistently until the difference in orbital populations between the initial and final states of the iteration was less than 0.01 electron/orbital. The computation details of the non-relativistic (DV-HFS) method used in the present work have been described elsewhere [49,50].

Acknowledgements

The authors would like to express their thanks to Professor I. Ikemoto and Dr. T. Kodama for a gift of fullerene samples. The authors wish to express their gratitude to Professor H. Adachi (Kyoto University) for permission to use a computational program. The authors also wish to thank Drs. H. Nakamatsu (Kyoto University) and R. Sekine (Shizuoka University) for fruitful discussions, useful technical advice and encouragement. The authors are grateful to Professors H. Imahori and Y. Sakata (Osaka University) for their kind advice for the syntheses of metal oeps. This research was supported partly by a Grant-in-Aid for Scientific Research on Priority Area (Nos. 10149104 and 11165235), 'Fullerenes and Nanotubes Networks' from the Ministry of Education, Science and Culture, Japan.

References

[1] C.A. Reed, R. Bolskar, Chem. Rev. 100 (2000) 1075.
[2] D. Konarev, R. Lyubovskaya, Russ. Chem. Rev. 68 (1999) 23.
[3] O.A. Dyachenko, A. Graja, Fullerene Sci. Tech. 7 (3) (1999) 317.
[4] M.J. Hardie, C.L. Raston, Chem. Commun. 0 (1999) 1153–1163.
[5] S.A. Olsen, A.M. Bond, R.G. Compton, G. Lazarev, P.J. Mahon, F. Marken, C.L. Raston, V. Tedesco, R. Webster, J. Phys. Chem. 102 (1998) 2641.
[6] K. Tsubaki, K. Tanaka, T. Kinoshita, K. Fuji, Chem. Commun. 0 (1998) 895.
[7] K.N. Rose, L.J. Barbour, G.W. Orr, J.L. Atwood, Chem. Commun. (1998) 407.
[8] Z. Yoshida, H. Takekuma, S. Takekuma, Y. Matsubara, Angew. Chem. Int. Ed. Engl. 33 (1994) 1597.
[9] F. Diedrich, J. Effing, U. Jonas, L. Jullien, T. Plesnivy, H. Ringsdorf, C. Thilgen, D. Weinstein, Angew. Chem. Int. Ed. Engl. 31 (1992) 1599.
[10] D.M. Eichhorn, S. Yang, W. Jarrell, T.F. Baumann, L.S. Beall, A.J.P. White, D.J. Williams, A.G.M. Barrett, B.M. Hoffman, J. Chem. Soc. Chem. Commun. (1995) 1703.
[11] D.M. Hochmuth, S.L.J. Michel, A.J.P. White, D.J. Williams, A.G.M. Barrett, B.M. Hoffman, Eur. J. Inorg. Chem. (2000) 593–596.
[12] J.W. Steed, P.C. Junk, J.L. Atwood, M.J. Barnes, C.L. Raston, R.S. Burkhalter, J. Am. Chem. Soc. 116 (1994) 10346.
[13] A. Izuoka, T. Tachikawa, T. Sugawara, Y. Suzuki, M. Konno, Y. Saito, H. Shinohara, J. Chem. Soc. Chem. Commun. (1992) 1472.
[14] D.V. Konarev, E.F. Valeev, Y.L. Slovokhotov, Y.M. Shul'ga, O.S. Roschupkina, R.N. Lyubovskaya, Synth. Met. 88 (1997) 85.
[15] P.D. Croucher, P.J. Nichols, C.L. Raston, J. Chem. Soc. Dalton Trans. (1999) 279.
[16] P.C. Andrews, J.L. Atwood, L.J. Barbour, P.J. Nichols, C.L. Raston, Chem. Eur. J. 4 (8) (1998) 1382.
[17] P.C. Andrews, J.L. Atwood, L.J. Barbour, P.D. Croucher, P.J. Nichols, N.O. Smith, B.W. Skelton, A.H. White, C.L. Raston, J. Chem. Soc. Dalton Trans. (1999) 2927.
[18] Y.-P. Sun, T. Drovetskaya, R.D. Bolskar, R. Bau, P.D.W. Boyd, C.A. Reed, J. Org. Chem. 62 (1997) 3642.
[19] M.M. Olmstead, D.A. Costa, K.M. Maitra, B.C. Noll, L. Phillips, P.M. Van Calcar, A.L. Balch, J. Am. Chem. Soc. 121 (1999) 7090–7097.
[20] P.D.W. Boyd, M.C. Hodgson, C.E.F. Rickard, A.G. Oliver, L. Chaker, P.J. Brothers, R.D. Bolskar, F.S. Tham, C.A. Reed, J. Am. Chem. Soc. 121 (1999) 10487–10495.

[21] The term '*anti*' in this paper denotes the *anti*-symmetry of the terminal eight ethyl groups on the porphyrin plane according to the *E*,*Z*-nomenclature. That is a different meaning from a so-called *anti*-compound mentioned in a review article by: A.L. Balch, et al., Chem. Rev. 98 (1998) 2123.

[22] J.M. Marshall, P.D. Croucher, P.J. Nichols, C.L. Raston, Chem. Commun. (1999) 193.

[23] T. Ishii, N. Aizawa, M. Yamashita, H. Matsuzaka, T. Kodama, K. Kikuchi, I. Ikemoto, Y. Iwasa, J. Chem. Soc. Dalton Trans. 23 (2000) 4407–4412.

[24] D.L. Cullen, E.F. Meyer Jr., Acta Crystallogr. Sect. B 32 (1976) 2259.

[25] M.O. Senge, T.P. Forsyth, K. Smith, Z. Kristallogr. 211 (1996) 176.

[26] T. Ishii, R. Kanehama, N. Aizawa, M. Yamashita, K. Sugiura, H. Miyasaka, T. Kodama, K. Kikuchi, I. Ikemoto, unpublished data.

[27] H.B. Burgi, R. Restori, D. Schwarzenbach, A.L. Balch, J.W. Lee, B.C. Noll, M.M. Olmstead, Chem. Mater. 6 (1994) 1325.

[28] A.M. Stolzenberg, L.J. Schussel, J.S. Summers, B.M. Foxman, J.L. Petersen, Inorg. Chem. 31 (1992) 1678–1686.

[29] R. Pak, W.R. Scheidt, Acta Crystallogr., Sect. C 47 (1991) 431–433.

[30] T. Ishii, N. Aizawa, R. Kanehama, M. Yamashita, H. Matsuzaka, T. Kodama, K. Kikuchi, I. Ikemoto, Inorg. Chim. Acta 317 (1–2) (2001) 81–90.

[31] T. Ishii, N. Aizawa, M. Yamashita, H. Matsuzaka, I. Ikemoto, K. Kikuchi, T. Kodama, Y. Iwasa, Synth. Met. 121 (2001) 1165.

[32] D.R. Evans, N.L.P. Fackler, Z. Xie, C.E.F. Rickard, P.W.D. Boyd, C.A. Reed, J. Am. Chem. Soc. 121 (1999) 8466 η^2-C_{60} cocrystallite = (5,10,15,20 - tetraphenylporphyrin) - (η^2 - C_{60})-iron(III)tetrakis(pentafluorophenyl)borate 1,2-dichlorobenzene solvate.

[33] T. Ishii, R. Kanehama, N. Aizawa, M. Yamashita, H. Matsuzaka, K. Sugiura, H. Miyasaka, T. Kodama, K. Kikuchi, I. Ikemoto, H. Tanaka, K. Marumoto, S.-I. Kuroda, J. Chem. Soc. Dalton Trans. 20 (2001) 2975–2980.

[34] A. Pénicaud, A. Peréz-Benítez, R. Gleason V., E. Muñoz P., R. Escudero, J. Am. Chem. Soc. 115 (1993) 10392–10393.

[35] T. Kodama, M. Kato, K. Mogi, M. Aoyagi, T. Kato, Mol. Phys. Rep. 18/19 (1997) 121–126.

[36] M.E. Kastner, W.R. Scheidt, J. Organomet. Chem. 157 (1978) 109.

[37] H. Masuda, T. Taga, H. Sugimoto, M. Mori, J. Organomet. Chem. 273 (1984) 385.

[38] J.S. Summers, J.L. Petersen, A.M. Stolzenberg, J. Am. Chem. Soc. 116 (1994) 7189.

[39] Y. Cao, J.L. Petersen, A.M. Stolzenberg, Inorg. Chim. Acta 263 (1997) 139.

[40] A.A. Gridnev, S.D. Ittel, B.B. Wayland, M. Fryd, Organometallics 15 (1996) 5116.

[41] S. Stevenson, G. Rice, T. Glass, K. Harich, F. Cromer, M.R. Jordan, J. Craft, E. Hadju, R. Bible, M.M. Olmstead, K. Maitra, A.J. Fisher, A.L. Balch, H.C. Dorn, Nature 401 (1999) 55–57.

[42] M.M. Olmstead, A. de Bettencourt-Dias, J.C. Duchamp, S. Stevenson, H.C. Dorn, A.L. Balch, J. Am. Chem. Soc. 122 (2000) 12220–12226.

[43] M.M. Olmstead, K. Maitra, A.L. Balch, Angew. Chem. Int. Ed. Engl. 38 (1999) 231.

[44] W.R. Scheidt, I. Turowska-Tyrk, Inorg. Chem. 33 (1994) 1314.

[45] T. Ishii, R. Sekine, T. Enoki, E. Miyazaki, T. Miyamae, T. Miyazaki, J. Phys. Soc. Jpn. 66 (11) (1997) 3424.

[46] C.S. Alexander, S.J. Rettig, B.R. James, Organometallics 13 (1994) 2542.

[47] F.R. Hopf, T.P. O'Brien, W.R. Scheidt, D.G. Whitten, J. Am. Chem. Soc. 97 (1975) 277.

[48] A. Rosen, D.E. Ellis, Chem. Phys. 62 (1975) 3039.

[49] H. Adachi, M. Tsukada, C. Satoko, J. Phys. Soc. Jpn. 45 (1978) 875.

[50] H. Nakamatsu, H. Adachi, T. Mukoyama, Bull. Inst. Chem. Res. Kyoto Univ. 70 (1992) 16.